SPATIAL FREQUENCY TUNED COVARIANCE CHANNELS UNDERLYING SCOTOPIC CONTRAST SENSITIVITY

PETERZELL, DAVID H.[1], **SCHEFRIN, BROOKE E.**[2], **TREGEAR, STEPHEN J.**[3], and **WERNER, JOHN S.**[4,2]

[1]University of California, San Diego, La Jolla, CA 92093 USA email: peterzel@psy.ucsd.edu
[2]University of Colorado, Boulder, CO 80309 USA email: brooke@psych.colorado.edu
[3]University of Colorado, Boulder, CO 80309 USA email: stregear@ecri.org
[4]University of California, Davis, CA 95817 USA email: jwerner@psych.colorado.edu

The processes underlying photopic contrast sensitivity functions (CSFs) have been modeled in terms of multiple channels selective for spatial frequency (De Valois & De Valois, 1988). The lowest frequency channel obtained foveally using stational sinusoidal gratings typically has its peak sensitivity near 1 c/deg (Greenlee et al. 1988; Peterzell & Teller, 1996, 2000; Tolhurst, 1973).

Less is known about the processes underlying scotopic contrast sensitivity. The channels underlying scotopic and photopic vision may differ considerably. Hess and Howell (1988) demonstrated that contrast sensitivity peaks near 0.2 c/deg when stimuli are presented at scotopic luminances. This low-frequency peak cannot be modeled using only a bandpass channel that peaks near 1 c/deg. Hence, the authors concluded that several spatial frequency channels exist at very low spatial frequencies but may operate at scotopic luminances only (or, similarly, the peak of a channel might shift to lower spatial frequencies at low light levels, due, perhaps, to a reduction of the influence of the surrounds of receptive fields). Greenlee et al. determined that the lowest adaptable frequency channel obtained using scotopic stationary gratings occurred well below 1 c/deg (as measured in rod monochromats). They concluded that rod monochromats differed from normals. Equally likely from their results, however, is the possibility that scotopic vision, unlike photopic vision, contains multiple spatial channels below 1 c/deg.

Over the last 15 years, about 20 psychophysical and electrophysiological studies with adults and infants have examined normal individual differences, using statistical covariance analyses in order to quantify the number of spatiotemporal channels, and to measure channels' spatial and temporal frequency tuning (reviews: Peterzell & Teller, 1996, 2000; Peterzell et al. 2000). The paradigm uses simple detection data to assess the unadapted, unmasked visual system. It requires relatively few complex theoretical assumptions or theoretical structure to estimate the number of channels, and provides a direct estimate of channel tuning. It has revealed mechanisms that map well onto channels derived using masking and adaptation.

Do the channels underlying scotopic CSFs differ from those underlying photopic CSFs? What is the number nature, and tuning of these spatial channels? The present study investigates these issues by analyzing 50 scotopic CSFs reported by Schefrin et al. (1999). Using covariance statistics, we identified the scotopic spatial channels and discovered that our results have important implications for theories of infant vision.

INDIVIDUAL DIFFERENCES THEORY

Fig. 1 is a schematic model of individual differences underlying CSFs. It illustrates the rationale for and assumptions of the paradigm.

Assumption 1: Multiple spatial channels exist. Panel 1 shows the sensitivities of 2 hypothetical channels that could exist in a subject. For simplicity, the model consists of only 2 channels. This subject's first channel (A, dashed line) is more sensitive at its peak than the second (B, solid line) at its peak.

Assumption 2: Channels determine CSF function shape. As shown in panel 2, Channels A and B mediate sensitivity below and above 2 c/deg, respectively. For simplicity, the function is deemed free of measurement error and a winner-take-all summation rule has been applied.

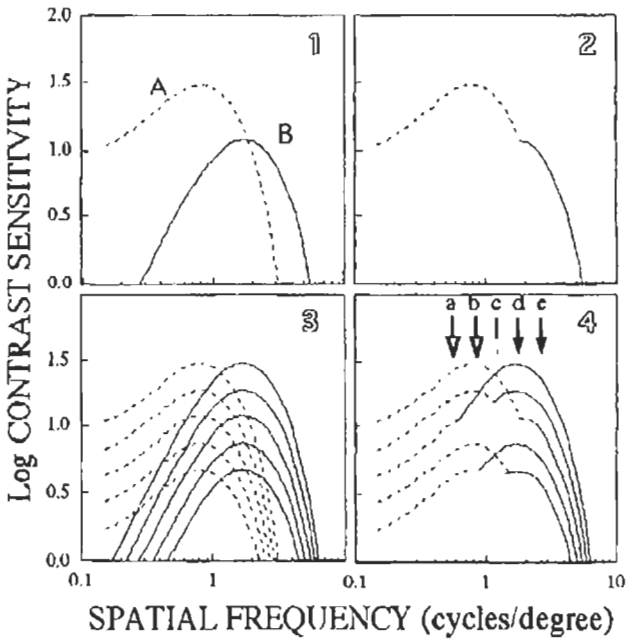

Assumption 3: Channel sensitivities vary independently across individuals; peak sensitivity of each channel is regularly distributed across subjects independent of the sensitivity of other channels. Panel 3 shows the Channels A and B, each at 5 different sensitivity levels. The subject in panel 1 has a highly sensitive Channel A and a Channel B of average sensitivity, based on the selection available in panel 3.

Implication 1: Individual variability in channel sensitivities can account for measurable individual variability in CSFs. This is illustrated in Panel 4, which shows CSFs for 5 hypothetical subjects. The 5 sensitivities measured at frequency *a* fall within a statistically regular (possibly normal) distribution. The 5 sensitivities measured at frequency *b* also fall within a statistically regular distribution, mappable, *with rank retention,* onto the distribution for *a*. This is due to the shared underlying channel (A). Likewise, the 5 sensitivities measured at frequency *d* fall within a distribution that is mappable, with rank retention, onto the distribution for spatial frequency *e*, as Channel B controls sensitivity at these frequencies. However, rank is not retained *across* the two distributions (*a,b* vs. *d,e*) because different channels control sensitivity. Frequency *c* represents the boundary region at which the two channels overlap, and is not fully determined by either channel.

Thus each subject retains his rank across the range of frequencies controlled by any one channel. The 5 sensitivities at one frequency correlate with those at similar but not dissimilar frequencies. For instance, the 5 sensitivities at frequency *a* correlate strongly with the 5 at frequency *b*, weakly with those at *c*, and not at all with those at *d* and *e*. This "selective correlational structure" describes the above relationships, which are akin to bandpass selectivity for spatial frequency.

Implication 2: Spatial channel characteristics can be inferred from individual differences in CSFs. Having assumed that individual variation in underlying channels contributes to individual variation in empirical CSFs, one can use individual differences in the functions to test and generate models of spatial channels (as described in earlier papers, and only briefly here).

METHODS: SCOTOPIC CSFs FROM SCHEFRIN ET AL. (1999).

Scotopic CSFs were measured for 50 observers between the ages of 20 and 88 years. Using a maximum-likelihood, 2-alternative, temporal forced-choice threshold-estimation algorithm, scotopic CSFs were measured at 7 spatial frequencies ranging from 0.2 to 3.0 c/deg, with mean retinal illuminance equated for observers at -0.85 log scotopic Trolands. For each stimulus condition, eight cycles of a horizontal sinusoidal grating were presented within a ± 1 S.D. of a 2-D Gaussian-spatial envelope and within a 1-s Gaussian-temporal envelope. Stimuli were centered on the nasal retina along the horizontal meridian 6° from the fovea.

Because only 3 subjects provided data at 3 c/deg, we excluded that point from our analyses. There is a tradeoff between the number of spatial frequencies and number of subjects included in our analyses. Thus, we analyzed a 12-subject data set (excluding 3 c/deg), a 37-subject data set (excluding 2.4, 3 c/deg), and a 50-subject data set (excluding 1.8, 2.4, 3 c/deg).

RESULTS

Mean CSFs. Fig. 2 shows the mean log scotopic contrast sensitivity as a function of spatial frequency. Consistent with previous studies, the scotopic CSF was lowpass (cf. Fiorentini & Maffei, 1973). The mean photopic CSF (Peterzell & Teller, 1996) provides a comparison.

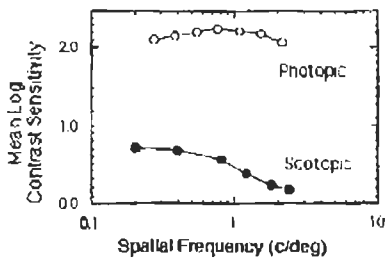

Channel tuning estimates from individual differences. Correlation matrices were calculated across the 12, 37 or 50 subjects for each spatial frequency against each other frequency (Table 1). Regions of high intercorrelations among sets of adjacent frequencies were found, suggesting the existence of sets of spatial frequencies that are detected by the same underlying channel. Statistical factor analyses, which derive variability sources (or *factors*) from the data, were then performed (following Peterzell & Teller, 1996, 2000). Because these statistics provided estimates of how many significant factors each data set contained, they were used to estimate the minimum number of spatial channels required to model the CSFs. Factor loadings (which describe correlations between a variable and a factor) were then used to estimate channel tuning. 2 or 3 factors were found in the data (depending on the size of the data set). All factors showed clear spatial frequency tuning; their loadings varied systematically with spatial frequency.

The tuning of channels was estimated by fitting the factor loadings to the scotopic contrast sensitivities (Fig 2). To do so, we used the following equation from Peterzell and Teller (1996):

$$\text{CHANNEL CONTRAST SENSITIVITY}_{in} = \frac{\text{MEAN LOG CONTRAST SENSITIVITY}_{n}}{(\text{abs}(1/\text{FACTOR LOADING}_{in}))^{1/Q}}$$

which determines the analyzer contrast sensitivity for factor*i* at spatial frequency *n*. *Q* is the exponent of an often used probability summation equation (Quick, 1974). *Q* was set to 4, consistent with results from photopic masking and channel theory (Wilson & Gelb, 1984). For each of the factors at each spatial frequency, Eq. 1 generated channel sensitivity values that can vary from near-zero (for factor loadings near zero) to the mean log contrast sensitivity (for factor loadings equal to one).

The symbols in Fig. 3 (lower panels) represent predicted contrast sensitivities that were calculated using Eq. 1, the mean log scotopic CSF (Fig. 1), and the factor loadings from the factor analyses described above. Each panel shows the predicted contrast sensitivities for one of the three scotopic data sets (12, 37 or 50 subjects). In each panel, the different symbols represent the predicted contrast sensitivities for the two or three significant statistical factors (or "covariance channels"). The symbols representing each covariance channel span a limited range of spatial frequencies. For comparison, the symbols in the upper panel show the two covariance channels obtained using low spatial frequencies presented under photopic conditions (Peterzell & Teller, 1996).

To clarify the implications of these results, the covariance channels (symbols) were compared to the channels (A and B) specified by a well known computational model of spatial vision, which was derived using photopic masking data (Wilson & Gelb, 1984). Channels A and B were fit to the mean CSFs in Fig. 2, as described previously (Peterzell & Teller, 1996). The results are shown by the solid curves in each panel. For the two scotopic channels tuned to the highest spatial frequencies, it is apparent (Fig. 3, lower panels) that the tuning functions resemble those obtained for photopic vision. That is, the symbols obtained from our data map onto the spatial channels (A and B) specified in the computational model. *In contrast to the photopic data, however, there exists a single covariance channel in the scotopic data that is tuned to very low spatial frequencies* , with a dashed line drawn through the points. This very low frequency channel was not predicted by the Wilson and Gelb (1984) model.

DISCUSSION

We have modeled the number and spatial tuning characteristics of spatial channels underlying the scotopic CSF. To do so, we examined the covariance structure of individual differences underlying 50 scotopic CSFs. We found evidence for 3 spatial channels operating below 3 c/deg, and estimated the spatial tuning functions for each channel.

Previous reports suggest that a single spatial channel (vs. multiple spatial channels) operates below 1 c/deg when the CSF is measured photopically with stationary gratings (Greenlee et al. 1988; Peterzell & Teller, 1996, 2000; Tolhurst, 1973). Our results do not contradict these reports, but indicate that for scotopic vision, an additional channel operates well below 1 c/deg. The lowest scotopic channel is not predicted by a computational model (Wilson & Gelb, 1984), whereas the other covariance channels coincide with model predictions (mechanisms A & B).

To the extent that we found evidence for multiple scotopic spatial channels below 1 c/deg, our results coincide with previous reports (Greenlee et al. 1988; Hess & Howell, 1988). We find, however, evidence for only 2 channels below 1 c/deg, in contrast to others who predicted a continuum of channels. We note that nothing in the previous reports supports the existence of a continuum vs. a discrete set of channels. In their adaptation experiment, Greenlee et al. (1988), made the common assumption that if maximal threshold elevation occurs at the frequency of the masking stimulus (i.e., "on-peak masking"), then the threshold elevation function must reflect channels tuned along a *continuum* of spatial frequencies. However, Tyler et al. (1993, 1994; Peterzell & Norcia, 1997) have shown that a model based on *discrete* channels can lead to on-peak masking or adaptation. Moreover, Greenlee et al. suggested that the very low frequency channel was unique to

Table 1
Correlations (r) Among Spatial Frequency Variables

	0.2	0.4	0.8	1.2	1.8
0.4	.86	(n=50)			
0.8	.63	.74			
1.2	.48	.60	.80		
0.4	.77	(n=37)			
0.8	.47	.64			
1.2	.22	.41	.75		
1.8	.21	.34	.60	.67	
0.4	.70	(n=12)			
0.8	.35	.37			
1.2	.48	.56	.52		
1.8	.46	.42	.37	.37	
2.4	.43	.47	.30	.42	.87

rod monochromats, a possibility not supported by the present study.

Our may have important implications for understanding the development of spatial channels. It is known that for stationary, photopic gratings, the coarsest spatial channel found in infants is tuned to a frequency well below the 1 c/deg value obtained from adults (review: Peterzell et al. 2000). A "scale change" hypothesis is typically used to explain this difference between adults and infants. It is believed that during development, the tuning of this and all other spatial channels shifts from lower to higher spatial frequencies by a factor of about 4, becoming adult-like sometime after 8 months postnatal. The shift is hypothesized to be caused by cone migration into the fovea and changes in eye size during development (Wilson, 1998).

Our results may provide an alternative to the developmental scale change hypothesis. Clavadetscher et al. (1988) and Brown (1990) suggested that rod initiated signals are more prominant in infants than adults (but see Chien et al. 1999). If infants' vision is rod dominated, then the multiple "shifting" channels observed during development may not reflect a spatial scale change due to anatomical changes. Rather, they may reflect a shift from rod- to cone-dominated vision as the infant's quantal efficiency increases with age.

Supported by NIA grant AG04058 (JSW) and NEI grant EY06706 (DHP)

REFERENCES

Brown, AM (1990). Development of visual sensitivity to light and color vision in human infants: A critical review. *Vision Research, 30*, 1159-1188.

Chien, H-L,Teller, DY & Palmer, JP (1999). "Rod dominance" in infants?: motion photometric measurements of the transition from scotopic to photopic vision in infants vs. adults. *IOVS suppl., 40*, S409.

Clavadetscher, JE, Brown, AM, Ankrum, C, & Teller, DY (1988). Spectral sensitivity and chromatic discriminations in 3- and 7-week-old human infants. *JOSA A, 5*, 2093-2105.

De Valois RL, De Valois KK (1988). *Spatial Vision*. NY: Oxford.

Fiorentini, A & Maffei, L (1973). Contrast in night vision. *Vision Research, 13*, 73-80.

Greenlee, MW, Magnussen, S & Nordby, K (1988). Spatial vision of the achromat: Spatial frequency and orientation - specific adaptation. *J. Physiology, 395*, 661-678.

Hess, RF & Howell, ER (1988). Detection of low spatial frequencies: A single filter or multiple filters? *Ophthalmic & Physiological Optics, 8*, 378-385.

Peterzell, DH, Chang, S, & Teller, DY (2000). Spatial frequency tuned *covariance* channels for red-green and luminance-modulated gratings: Psychophysical data from human infants. In Press, *Vision Research*.

Peterzell, DH & Norcia, AM (1997). Spatial frequency masking with the sweep-VEP. *Vision Research, 37*, 2349-2359.

Peterzell, DH & Teller, DY (1996). Individual differences in contrast sensitivity functions: the lowest spatial frequency channels. *Vision Research, 20*, in press.

Peterzell, DH & Teller, DY (2000). Spatial frequency tuned covariance channels for red-green and luminance-modulated gratings: Psychophysical data from human adults. In press, *Vision Research*.

Quick, RF (1974). A vector-magnitude model of contrast detection. *Kybernetik, 16*, 65-67.

Schefrin, BE, Tragear, SJ, Harvey, LO, Jr, & Werner, JS (1999). Senescent changes in scotopic contrast sensitivity. *Vision Research, 39*, 3728-3736.

Tolhurst, D (1973). Separate channels for the analysis of the shape and movement of a moving visual stimulus. *Journal of Physiology, 231*, 385-402.

Tyler, CW, Barghout, L, & Kontsevich, LL (1993). Surprises in analyzing the mechanisms underlying threshold elevation functions. *Investigative Ophthalmology and Visual Science (Suppl.), 34*, 819.

Tyler, CW, Barghout, L, & Kontsevich, LL (1994). Computational reconstruction of the mechanisms of human stereopsis. In TB Lawton (Ed), *Computational vision based on neurobiology, Proc. SPIE 2054*, 52-68.

Wilson, HR (1988). Development of spatiotemporal mechanisms in infant vision. *Vis Res 28*, 611-628

Wilson, HR & Gelb, DJ (1984). Modified line element theory for spatial frequency and width discrimination. *JOSA, A1*, 124-131.

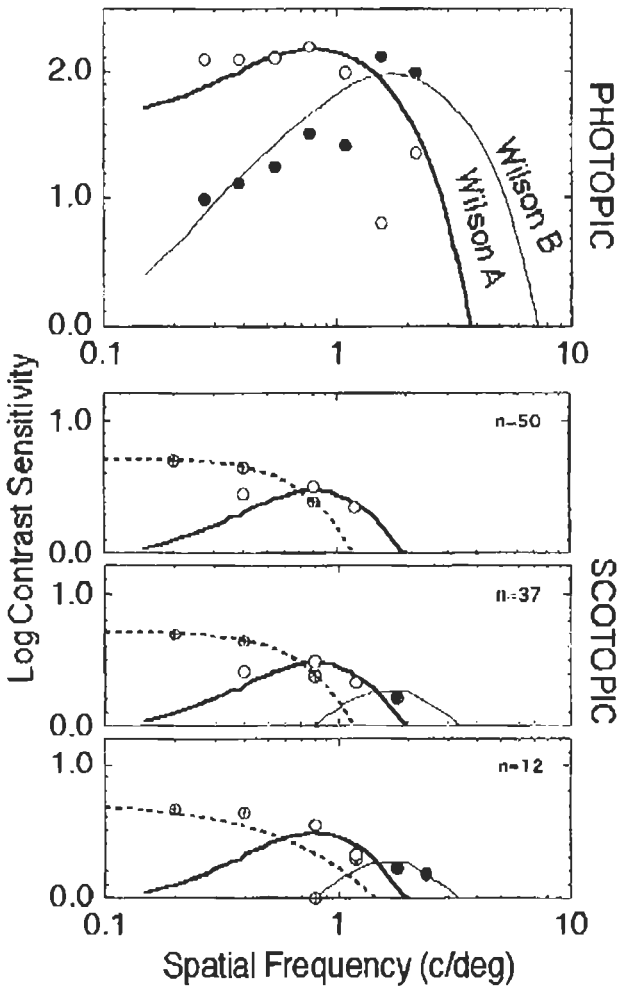

FB3 11:25am
Contextual deployment of attention in driving, *Hiroyuki Shinoda, Ritsumeikan Univ., Japan; Mary M. Hayhoe, Anurag Shrivastava, Dana H. Ballard, Univ. of Rochester, USA*
We examined the detectability of a STOP sign placed in two different contexts, either in the mid-block or at an intersection, in a virtual environment. High detectability at the intersection and low in the mid-block indicate that visual system deploys attention using contextual cues in natural and complex tasks. **(p. 29)**

Discussant: *Kent E. Higgins, Lighthouse Intl., USA*

11:50am–1:30pm
Lunch Break (on your own)

1:30pm–3:10pm
Room: Anasazi
FC ■ Visual Mechanisms
Elisabeth M. Fine, Schepens Eye Res. Inst., USA, Presider

FC1 1:30pm
Detecting and discriminating curved gabors for static, drifting, and warping stimuli, *Jocelyn Faubert, Michel Pinard, Pierre Simonet, Jacques Gresset, Univ. de Montréal, Canada*
We assessed detection and discrimination for curved Gabors in order to make predictions about the potential impact optical distortions may have on visual performance. **(p. 35)**

Discussant: *Nancy J. Coletta, New England Col. of Optometry, USA*

FC2 1:55pm
Spatial frequency tuned covariance channels underlying scotopic contrast sensitivity, *David H. Peterzell, Univ. of California-San Diego, USA; Brooke E. Schefrin, Stephen J. Tregear, Univ. of Colorado, USA; John S. Werner, Univ. of California–Davis, USA*
Covariance structure analyses of scotopic contrast sensitivity functions (from 50 subjects) revealed the existence and tuning of three discrete spatial channels. Two channels coincide with Wilson's model. A third is tuned to well below 1 c/deg. **(p. 39)**

Discussant: *Kenneth R. Alexander, Univ. of Illinois–Chicago, USA*

FC3 2:20pm
Blood flow responses of the human optic nerve to luminance and chromatic flicker: correlation with magno- and parvocellular neural activity, *Charles E. Riva, Inst. de Recherche en Ophtalmologie and Univ. Lausanne, Switzerland; Benedetto Falsini, Catholic Univ., Italy; Eric Logean, Inst. de Recherche en Ophtalmologie, Switzerland*
Using laser Doppler flowmetry, we measured the optic nerve blood flow response (DF) to red-green counter-phased flicker varying in color ratio and temporal frequency. DF displayed physiological properties similar to magno- and parvo-cellular systems' responses. **(p. 43)**

Discussant: *John Werner, Univ. of California–Davis, USA*

FC4 2:45pm
Local and global visual function deficits in patients with ABCR gene mutations, *Yi-Zhong Wang, David G. Birch, Retina Foundation of the Southwest, USA*
Stargardt's patients have a significant decrease in global hyperacuity while still retaining relatively good visual acuity, suggesting global hyperacuity is more sensitive than visual acuity for quantifying early visual loss from macular degeneration. **(p. 47)**

Discussant: *Stanley Klein, Univ. of California–Berkeley, USA*

3:10pm–3:30pm
Room: Concourse
Coffee Break

3:30pm–5:10pm
Room: Anasazi
FD ■ ERGs and Disease
David G. Birch, Retina Foundation of Southwest, USA, Presider

FD1 3:30pm
Visual function in patients with cone-rod dystrophy (CRD) associated with ABCR gene mutations, *D.G. Birch, A.Y. Peters, K.L. Locke, Retina Foundation of the Southwest, USA; C.F. Megarity, G.H. Travis, Univ. Texas Health Center, USA*
Mutations in the ABCR gene cause recessive Stargardt disease. In this study, we investigate the possibility that mutations in ABCR are associated with recessive cone-rod dystrophy (CRD) and use psychophysical, electroretinographic, and pupillometric techniques to characterize the phenotype. **(p. 53)**

Discussant: *Joseph M. Harrison, Univ. of Texas–San Antonio, USA*